Journal of Sound and Vibration (1972) **25** (1), 111–128

DIGITAL SIMULATION OF RANDOM PROCESSES AND ITS APPLICATIONS

M. SHINOZUKA

Department of Civil Engineering and Engineering Mechanics, Columbia University, New York, New York 10027, *U.S.A.*

AND

C.-M. JAN

Gibbs and Hill Inc., New York, New York 10027, *U.S.A.*

(*Received* 10 *April* 1972, *and in revised form* 17 *August* 1972)

Efficient methods are presented for digital simulation of a general homogeneous process (multidimensional or multivariate or multivariate-multidimensional) as a series of cosine functions with weighted amplitudes, almost evenly spaced frequencies, and random phase angles. The approach is also extended to the simulation of a general non-homogeneous oscillatory process characterized by an evolutionary power spectrum. Generalized forces involved in the modal analysis of linear or non-linear structures can be efficiently simulated as a multivariate process using the cross-spectral density matrix computed from the spectral density function of the multidimensional excitation process. Possible applications include simulation of (i) wind-induced ocean wave elevation, (ii) spatial random variation of material properties, (iii) the fluctuating part of atmospheric wind velocities and (iv) random surface roughness of highways and airport runways.

1. INTRODUCTION

The recent advent of high speed digital computers has made it practical to apply the so-called Monte Carlo techniques to a much larger variety of engineering problems than ever before. In the present study, a particular effort is made to develop a technique of digital simulation of multivariate or multidimensional or multivariate-multidimensional random processes which can be used as an essential tool in a general Monte Carlo method of solution for a large number of problems in structural engineering. For example, the method can be used in (a) numerical analysis of dynamic response of non-linear structures to random excitations, (b) time domain analysis of linear structures under random excitations performed for the purpose of obtaining a kind of information, such as first excursion probability and exact time history of a sample function, that is not obtainable from the standard frequency domain analysis, and (c) numerical solution of stress wave propagation through a random medium and eigenvalue problems of structures with randomly non-homogeneous material properties.

Numerous papers dealing with simulations of a random process have been published in recent years (see, for example, references [1–7]). Only in the papers by Shinozuka [1] and Borgman [2], however, were methods proposed for simulating a random process of more than a single dimension or a single component.

In the simulation of ocean surface elevation, Borgman used wave superposition by choosing the frequency in such a way that the amplitude of each (sinusoidal) wave function was an equal portion of the cumulative spectrum. Borgman also presented a method for simulating several simultaneous time series by passing a white noise vector through filters.

The essential feature of Shinozuka's approach [1] is that a random process can be simulated by a series of cosine functions with random frequency (or wave number). The density function (or joint density function) of the random frequency is derived from the specified cross-spectral density matrix for multivariate process or from the specified spectral density function for multidimensional process. For example, a three-dimensional homogeneous Gaussian process, $f(x_1, x_2, x_3)$, with its spectral density function, $s_0(\omega_1, \omega_2, \omega_3)$, specified, can be simulated by

$$f(x_1, x_2, x_3) = \sigma \left(\frac{2}{N}\right)^{\frac{1}{2}} \sum_{k=1}^{N} \cos(\omega_{1k} x_1 + \omega_{2k} x_2 + \omega_{3k} x_3 + \phi_k), \tag{1}$$

with ϕ_k being the independent random variable uniformly distributed between 0 and 2π and with $\omega_{1k}, \omega_{2k}, \omega_{3k}$ being the random frequencies distributed according to the joint density function

$$g(\omega_1, \omega_2, \omega_3) = s_0(\omega_1, \omega_2, \omega_3)/\sigma^2,$$

where

$$\sigma^2 = \int_{-\infty}^{\infty} \int_{-\infty}^{\infty} \int_{-\infty}^{\infty} s_0(\omega_1, \omega_2, \omega_3)\, d\omega_1\, d\omega_2\, d\omega_3.$$

The process simulated in terms of equation (1) is ergodic as $N \to \infty$, and the simulated spectral density converges as $1/\sqrt{N}$ in the mean square sense to the target spectral density. This method of simulation has recently been applied successfully to a variety of engineering problems [8–11].

When the dimensionality of the process is large and the spectral distribution is not obtainable in closed form, however, the generation of random frequencies is very time consuming. In the present study, the previous approach [1] is improved by simulating a random process as a series of cosine functions with weighted amplitudes and almost evenly spaced frequencies. As a result, the rate of convergence is increased, and thus the time required to simulate a process is reduced, which is the key to a success of the Monte Carlo solution.

While in reference [1] the techniques were presented only for the simulation of a multidimensional or a multivariate homogeneous process, in this second phase of the study, the previous approach is not only modified to improve its efficiency in terms of simulation time but also is extended so that the simulation of a multivariate-multidimensional homogeneous process or a multidimensional non-homogeneous process is now possible.

In performing either the normal mode analysis of linear structures or the modal analysis of non-linear structures in a Galerkin sense, one always deals with generalized forces. When the excitation is of random nature, then the simulation of a generalized force plays an important role in the numerical solution, especially to the non-linear problems. In fact, a method is also presented by which such generalized forces can be effectively simulated as a multivariate process by using the cross-spectral density matrix computed from the spectral functions of the multidimensional excitation processes.

The usefulness of this proposed method of simulation has been demonstrated in a number of recent papers [12–16].

2. SIMULATION OF A MULTIDIMENSIONAL HOMOGENEOUS PROCESS

The autocorrelation function of an n-dimensional homogeneous real process $f_0(\mathbf{x})$, defined by

$$R_0(\xi) = E[f_0(\mathbf{x}_1) f_0(\mathbf{x}_2)],$$

where $\mathbf{x}_1$ and $\mathbf{x}_2$ are space vectors and $\xi = \mathbf{x}_2 - \mathbf{x}_1$ is the separation vector, is even in ξ (symmetric with respect to the origin of the n-dimensional space):

$$R_0(\xi) = R_0(-\xi). \tag{2}$$

Assume that the n-fold Fourier transform of $R_0(\xi)$ exists. The spectral density function of $f_0(\mathbf{x})$ is then defined as

$$S_0(\boldsymbol{\omega}) = \frac{1}{(2\pi)^n} \int_{-\infty}^{\infty} R_0(\xi)\, e^{-i\boldsymbol{\omega}\cdot\xi}\, d\xi, \tag{3}$$

where $\boldsymbol{\omega}$ is the frequency (wave number) vector and $\boldsymbol{\omega}\cdot\xi$ is the inner product of $\boldsymbol{\omega}$ and ξ, and, for simplicity

$$\int_{-\infty}^{\infty} (\quad)\, d\xi \equiv \int_{-\infty}^{\infty} \overset{n\text{-fold}}{\cdots\cdots} \int_{-\infty}^{\infty} (\quad)\, d\xi_1\, d\xi_2 \ldots d\xi_n,$$

with n being the dimension of the vector ξ. It follows from equation (2) that

$$\int_{-\infty}^{\infty} R_0(\xi) \sin(\boldsymbol{\omega}\cdot\xi)\, d\xi = 0$$

and also, from equation (3),

$$S_0(\boldsymbol{\omega}) = S_0(-\boldsymbol{\omega}).$$

Then

$$S_0(\boldsymbol{\omega}) = \frac{1}{(2\pi)^n} \int_{-\infty}^{\infty} R_0(\xi) \cos(\boldsymbol{\omega}\cdot\xi)\, d\xi \tag{4}$$

and is real.

For an arbitrary function $\rho(\mathbf{x})$ and an arbitrary n-dimensional domain of integration D_n, it can be shown that

$$\int_{D_n}\int_{D_n} R_0(\mathbf{x}_2 - \mathbf{x}_1)\, \rho(\mathbf{x}_1)\, \rho(\mathbf{x}_2)\, d\mathbf{x}_1\, d\mathbf{x}_2 = E\left[\int_{D_n} f_0(\mathbf{x}_1)\, \rho(\mathbf{x}_1)\, d\mathbf{x}_1\right]^2 \geqslant 0.$$

Therefore the autocorrelation function $R_0(\xi)$ is non-negative definite, and, according to Bochner [17], it has a non-negative n-fold Fourier transform: i.e.,

$$S_0(\boldsymbol{\omega}) \geqslant 0.$$

Based on these properties of $S_0(\boldsymbol{\omega})$, an efficient method of simulating $f_0(\mathbf{x})$ is proposed in the following.

Consider an n-dimensional homogeneous process with mean zero and spectral density function $S_0(\boldsymbol{\omega})$ which is of insignificant magnitude outside the region defined by

$$-\infty < \boldsymbol{\omega}_l \leqslant \boldsymbol{\omega} \leqslant \boldsymbol{\omega}_u < \infty,$$

where usually $\boldsymbol{\omega}_l = -\boldsymbol{\omega}_u$. Denote the interval vector by

$$(\Delta\omega_1, \Delta\omega_2, \ldots, \Delta\omega_n) = \frac{\omega_{1u} - \omega_{1l}}{N_1}, \frac{\omega_{2u} - \omega_{2l}}{N_2}, \ldots, \frac{\omega_{nu} - \omega_{nl}}{N_n},$$

with N_i being the number of intervals along the ith axis of the wave number domain. Then

the process can be simulated by the series

$$f(\mathbf{x}) = \sqrt{2} \sum_{k_1=1}^{N_1} \sum_{k_2=1}^{N_2} \cdots \sum_{k_n=1}^{N_n} [S_0(\omega_{1k_1}, \omega_{2k_2} \ldots \omega_{nk_n}) \, \Delta\omega_1 \, \Delta\omega_2 \ldots \Delta\omega_n]^{\frac{1}{2}}$$

$$\cos(\omega'_{1k_1} x_1 + \omega'_{2k_2} x_2 + \ldots + \omega'_{nk_n} x_n + \phi_{k_1 k_2 \ldots k_n}), \tag{5}$$

where

$\phi_{k_1 k_2 \ldots k_n}$ = independent random phase uniformly distributed between 0 and 2π,

$\omega_{ik_i} = \omega_{il} + (k_i - \frac{1}{2}) \Delta\omega_i, \quad k_i = 1, 2, \ldots, N_i, \quad i = 1, 2, \ldots n,$

$\omega'_{ik_i} = \omega_{ik_i} + \delta\omega_i, \qquad k_i = 1, 2, \ldots, N_i, \quad i = 1, 2, \ldots n,$

in which $\delta\omega_i$ is a small random frequency introduced to avoid the periodicity of the simulated process, and is uniformly distributed between $-\Delta\omega_i'/2$ and $\Delta\omega_i'/2$ with $\Delta\omega_i' \ll \Delta\omega_i$.

To avoid the lengthy expressions in the subsequent discussion, equation (5) will be written in the following compact form:

$$f(\mathbf{x}) = \sqrt{2} \sum_{k=1}^{N} A(\boldsymbol{\omega}_k) \cos(\boldsymbol{\omega}_k' \cdot \mathbf{x} + \phi_k), \tag{5a}$$

where

$$N = N_1 N_2 \ldots N_n, \; A(\boldsymbol{\omega}_k) = [S_0(\boldsymbol{\omega}_k) \, \Delta\omega_1 \, \Delta\omega_2 \ldots \Delta\omega_n]^{\frac{1}{2}} = [S_0(\boldsymbol{\omega}_k) \, \Delta\boldsymbol{\omega}]^{\frac{1}{2}}.$$

It is noted that if the symmetric condition of $S_0(\boldsymbol{\omega})$ is used, N in equation (5) can be reduced by one-half. Furthermore, if the process is isotropic, N is reduced to $N/2^n$.

It is easy to show that the ensemble average of $f(\mathbf{x})$ is zero. The autocorrelation function $R(\boldsymbol{\xi})$ of $f(\mathbf{x})$ becomes

$$\begin{aligned} R(\boldsymbol{\xi}) &= E[f(\mathbf{x}) f(\mathbf{x} + \boldsymbol{\xi})] \\ &= \sum_{k=1}^{N} A^2(\boldsymbol{\omega}_k) \, E[\cos(\boldsymbol{\omega}_k' \cdot \boldsymbol{\xi})] \\ &= \sum_{k=1}^{N} A^2(\boldsymbol{\omega}_k) \int_{-\frac{1}{2}\Delta\omega_n'}^{\frac{1}{2}\Delta\omega_n'} \frac{1}{\Delta\omega_n'} \int_{-\frac{1}{2}\Delta\omega_{n-1}'}^{\frac{1}{2}\Delta\omega_{n-1}'} \frac{1}{\Delta\omega_{n-1}'} \cdots \int_{-\frac{1}{2}\Delta\omega_1'}^{\frac{1}{2}\Delta\omega_1'} \frac{1}{\Delta\omega_1'} \\ &\qquad \times \cos(\boldsymbol{\omega}_k' \cdot \boldsymbol{\xi}), \, \mathrm{d}(\delta\omega_1) \ldots \mathrm{d}(\delta\omega_{n-1}) \, \mathrm{d}(\delta\omega_n). \end{aligned} \tag{6}$$

Note that $\boldsymbol{\omega}_k' \cdot \boldsymbol{\xi}$ can be written as

$$\boldsymbol{\omega}_k' \cdot \boldsymbol{\xi} = (\omega'_{1k_1} + \delta\omega_1) \, \xi_1 + \boldsymbol{\omega}'_{k_{n-1}} \cdot \boldsymbol{\xi}_{n-1}$$

with $\boldsymbol{\omega}'_{k_{n-1}} = (\omega'_{2k_2}, \omega'_{3k_3}, \ldots \omega'_{nk_n})$, and $\boldsymbol{\xi}_{n-1} = (\xi_2, \xi_3, \ldots \xi_n)$. By trigonometric expansion and the assumption that $\Delta\omega_1' \, \xi_1 \ll 1$, it can be shown that

$$\int_{-\frac{1}{2}\Delta\omega_1'}^{\frac{1}{2}\Delta\omega_1'} \frac{1}{\Delta\omega_1'} \cos(\boldsymbol{\omega}_k' \cdot \boldsymbol{\xi}) \, \mathrm{d}(\delta\omega_1) = \cos(\omega_{k_1} \xi_1 + \boldsymbol{\omega}_{k_{n-1}} \cdot \boldsymbol{\xi}_{n-1}). \tag{7}$$

Thus by successive application of equation (7), equation (6) is reduced to

$$R(\boldsymbol{\xi}) = \sum_{k=1}^{N} A^2(\boldsymbol{\omega}_k) \cos(\boldsymbol{\omega}_k \cdot \boldsymbol{\xi}). \tag{8}$$

Upon substituting $A^2(\omega_k) = S_0(\omega_k)\,\Delta\omega$, and taking the limit as $N \to \infty$ (in the sense that $N_1, N_2, \ldots, N_n \to \infty$ simultaneously) one obtains

$$R(\xi) = \int_{-\infty}^{\infty} S_0(\omega) \cos(\omega \cdot \xi)\, d\omega = R_0(\xi), \tag{9}$$

where it is assumed that $S_0(\omega) = 0$ for $\omega < w_l$ and $\omega > \omega_u$.

This indicates that, when the ensemble average is considered, the simulated process $f(\mathbf{x})$ possesses the target autocorrelation $R_0(\xi)$ and therefore the target spectral density $S_0(\omega)$.

The temporal (spatial) mean $\langle f(\mathbf{x})\rangle$ is zero since it can be shown that

$$|f(\mathbf{x})| = \left| \lim_{L_1, L_2, \ldots, L_n \to \infty} \sqrt{2} \sum_{k=1}^{N} \frac{A(\omega_k)}{L_1 L_2 \ldots L_n} \int_{-\frac{1}{2}L_n}^{\frac{1}{2}L_1} \ldots \int_{-\frac{1}{2}L_n}^{\frac{1}{2}L_n} \cos(\omega_k' \cdot \mathbf{x} + \phi_k)\, dx_1 \ldots dx_n \right|$$

$$\leqslant \lim_{L_1, L_2, \ldots, L_n \to \infty} 2^n \sqrt{2} \sum_{k=1}^{N} \frac{A(\omega_k)}{L_1 L_2 \ldots L_n \bar{\omega}_1 \bar{\omega}_2 \ldots \bar{\omega}_n} = 0, \tag{10}$$

where $\bar{\omega}_i$ is the smallest of $\omega_{ik_i} (k_i = 1, 2, \ldots N_i)$.

For simplicity of notation, ω_k' and ϕ_k are not considered as random variables but are treated as sample values of these random variables when dealing with the temporal averages.

The temporal (spatial) autocorrelation $R^*(\xi) = \langle f(\mathbf{x}) f(\mathbf{x} + \xi)\rangle$ becomes

$$R^*(\xi) = \lim_{L_1, \ldots, L_n \to \infty} \frac{2}{L_1 L_2 \ldots L_n} \sum_{k=1}^{N} \sum_{l=1}^{N} A(\omega_k) A(\omega_l) \int_{-\frac{1}{2}L_1}^{\frac{1}{2}L_1} \ldots \int_{-\frac{1}{2}L_n}^{\frac{1}{2}L_n}$$

$$\times [\cos(\omega_k' \cdot \mathbf{x} + \phi_k) \cos(\omega_l' \cdot \mathbf{x} + \omega_l' \cdot \xi + \phi_l)]\, dx_1 \ldots dx_n$$

$$= \sum_{k=1}^{N} A^2(\omega_k) \cos(\omega_k' \cdot \xi).$$

Using once again the assumption that $\Delta\omega' \cdot \xi < 1$, one obtains

$$R^*(\xi) = \sum_{k=1}^{N} A^2(\omega_k) \cos(\omega_k \cdot \xi). \tag{11}$$

As $N \to \infty$, equation (11) becomes

$$R^*(\xi) = \int_{-\infty}^{\infty} S_0(\omega) \cos(\omega \cdot \xi)\, d\omega = R_0(\xi). \tag{12}$$

The process simulated by the technique presented in reference [1] is ergodic only at $N \to \infty$. From equations (8) and (11), however, it is seen that the process $f(\mathbf{x})$ in equation (5) is ergodic regardless of the size of N. This makes the method directly applicable to a time domain analysis in which the ensemble average can be evaluated in terms of the temporal average. Note that the simulated process is Gaussian by virtue of the central limit theorem.

It is also shown in Appendix I that both the auto-correlation and spectral density functions of the simulated process converge as $1/N^2$ to the target auto-correlation function and the target spectral density function, respectively. The improvement in convergence from $1/\sqrt{N}$ (in reference [1]) to $1/N^2$ results in a remarkable reduction in computer time.

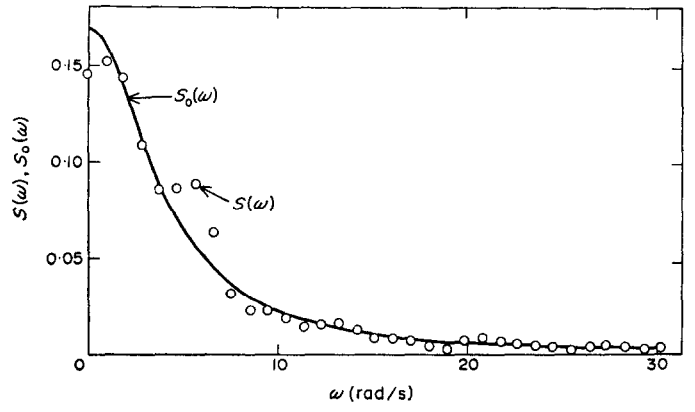

Figure 1. Target and simulated spectra. $S_0(\omega) = \left[\tan^{-1}\frac{\omega_0}{\alpha}\right]^{-1}\frac{\alpha}{\omega^2+\alpha^2}$; $\omega_0 = 12\pi$ rad/s; $\alpha = 4$ rad/s. $f(t) = \sqrt{\frac{2}{N}}\sum_{k=1}^{N}\cos(\omega_k t + \phi_k)$ with $N = 500$; ω_k = random frequency.

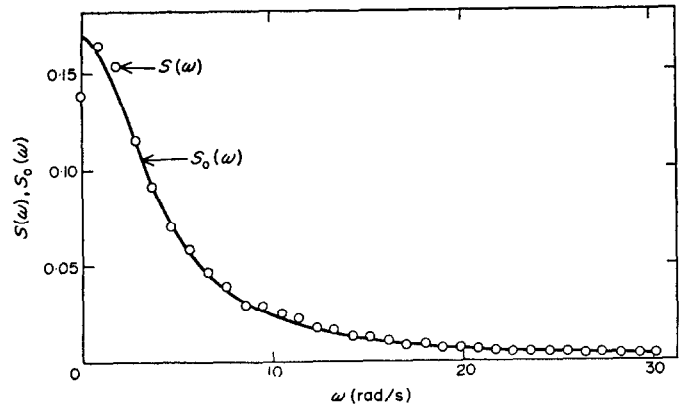

Figure 2. Target and simulated spectra. $f(t) = \sqrt{2}\sum_{k=1}^{N}[S_0(\omega_k)\Delta\omega]^{\frac{1}{2}}\cos(\omega_k' t + \phi_k)$ with $N = 50$; $\Delta\omega' = \frac{1}{20}\Delta\omega$.

For the purpose of comparison, a one-dimensional process $f(t)$ was simulated, by two different techniques, from a normalized one sided target spectral density,

$$S_0(\omega) = S_0\frac{\alpha}{\alpha^2+\omega^2}, \qquad 0 \leqslant \omega \leqslant \omega_u, \tag{13}$$

where

$$S_0 = \left[\tan^{-1}\frac{\omega_u}{\alpha}\right]^{-1}, \qquad \omega_u = 12\pi \text{ rad/s},$$

and $\alpha = 4$ rad/s. The process is first simulated, according to equation (1), by

$$f(t) = \sqrt{\frac{2}{N}}\sum_{k=1}^{N}\cos(\omega_k t + \phi_k), \tag{14}$$

with $N = 500$. It is assumed that the N so chosen is large enough so that the simulated process is approximately ergodic. The simulated spectral density is then obtained by taking the Fourier transform of the temporal auto-correlation. The result is plotted (open circles) in Figure 1 in which the target spectral density is also shown (solid curve). The process is then simulated, according to equation (5), by

$$f(t) = \sqrt{2} \sum_{k=1}^{N} [S_0(\omega_k)\, \Delta\omega]^{\frac{1}{2}} \cos(\omega_k' t + \phi_k) \tag{15}$$

with $N = 50$ and $\Delta\omega' = \Delta\omega/20$. The corresponding result is plotted in Figure 2. It is immediately seen that the result is much better for the latter case although the number of terms in the series is only one-tenth of the former one. For this particular example, the times required to simulate 5000 points of $f(t)$ are 58 s and 8 s, respectively.

At this point, it is parenthetically stated that the representation of one-dimensional one-variate random process in the form of equation (15) appeared in reference [18].

3. SIMULATION OF MULTIVARIATE MULTIDIMENSIONAL HOMOGENEOUS PROCESSES

Consider a set of m homogeneous Gaussian n-dimensional processes $f_j^0(\mathbf{x})$ $(j = 1, 2, \ldots m)$ with mean zero and with the cross-spectral density matrix $S^0(\boldsymbol{\omega})$ defined by

$$\begin{bmatrix} S_{11}^0(\boldsymbol{\omega}) & S_{12}^0(\boldsymbol{\omega}) \ldots S_{1m}^0(\boldsymbol{\omega}) \\ S_{21}^0(\boldsymbol{\omega}) & S_{22}^0(\boldsymbol{\omega}) \ldots S_{2m}^0(\boldsymbol{\omega}) \\ \ldots\ldots\ldots\ldots\ldots\ldots\ldots \\ S_{m1}^0(\boldsymbol{\omega}) & S_{m2}^0(\boldsymbol{\omega}) \ldots S_{mm}^0(\boldsymbol{\omega}) \end{bmatrix}$$

where $S_{jk}^0(\boldsymbol{\omega})$ is the n-fold Fourier transform of the cross correlation $R_{j_k}^0(\boldsymbol{\xi})$.

Due to the fact that $R_{jk}^0(\boldsymbol{\xi}) = R_{kj}^0(-\boldsymbol{\xi})$, one obtains

$$S_{jk}^0(\boldsymbol{\omega}) = \bar{S}_{kj}^0(\boldsymbol{\omega}), \tag{16}$$

where the bar indicates the complex conjugate.

The matrix $S^0(\boldsymbol{\omega})$ is therefore Hermitian. As in the case of a one-dimensional multivariate process [19], it can be shown that the matrix $S^0(\boldsymbol{\omega})$ is also non-negative definite. To prove this, construct a process $g^0(\mathbf{x})$,

$$g^0(\mathbf{x}) = \sum_{j=1}^{m} C_j f_j^0(\mathbf{x}),$$

with the C_j being arbitrary constants. The autocorrelation function of $g^0(\mathbf{x})$ becomes

$$R_g{}^0(\boldsymbol{\xi}) = \sum_{j=1}^{m} \sum_{k=1}^{m} C_j C_k R_{jk}^0(\boldsymbol{\xi}).$$

Introducing the Wiener–Khintchine relationship on both $R_g{}^0(\boldsymbol{\xi})$ and $R_{jk}^0(\boldsymbol{\xi})$ yields

$$\sum_{j=1}^{m} \sum_{k=1}^{m} C_j C_k S_{jk}^0(\boldsymbol{\omega}) = S_g{}^0(\boldsymbol{\omega}) \geqslant 0,$$

where the non-negativeness follows since $g^0(\mathbf{x})$ is also a homogeneous process. Therefore, $S^0(\boldsymbol{\omega})$ is non-negative definite.

Suppose one can find a matrix $H(\boldsymbol{\omega})$ which possesses an n-dimensional Fourier transform

and satisfies the equation

$$S^0(\omega) = H(\omega)\,\overline{H}(\omega)^T, \tag{17}$$

where $S^0(\omega)$ is the specified target cross-spectral matrix and T indicates the transpose. Then $f_j(\mathbf{x})$ $(j = 1, 2, \ldots, m)$ can be simulated by the following filtering technique:

$$f_j(\mathbf{x}) = \sum_{k=1}^{m} \int_{-\infty}^{\mathbf{x}} h_{jk}(\mathbf{x} - \xi)\,\eta_k(\xi)\,d\xi, \tag{18}$$

where $h_{jk}(\mathbf{x})$ is the n-dimensional Fourier transform of $H_{jk}(\omega)$,

$$h_{jk}(\mathbf{x}) = \int_{-\infty}^{\infty} H_{jk}(\omega) \exp(-i\omega \cdot \mathbf{x})\,d\omega,$$

and $\eta_k(\mathbf{x})$ is an independent n-dimensional normalized white noise component such that

$$E[\eta_j(\mathbf{x}_1)\,\eta_k(\mathbf{x}_2)] = \delta(\mathbf{x}_1 - \mathbf{x}_2)\,\delta_{jk},$$

with

$$\delta(\mathbf{x}_1 - \mathbf{x}_2) = \delta(x_{11} - x_{21})\,\delta(x_{12} - x_{22}) \ldots \delta(x_{1n} - x_{2n}).$$

It can be easily verified that the $f_j(\mathbf{x})$ $(j = 1, \ldots m)$, as simulated by equation (18), satisfy equation (17) and thus represent the target processes.

To find the matrix $H(\omega)$ in an efficient way, one can assume that $H(\omega)$ is a lower triangular matrix:

$$H(\omega) = \begin{bmatrix} H_{11}(\omega) & 0 & 0 & \ldots & 0 \\ H_{21}(\omega) & H_{22}(\omega) & . & \ldots & 0 \\ \ldots & \ldots & \ldots & \ldots & \ldots \\ H_{m1}(\omega) & H_{m2}(\omega) & . & \ldots & H_{mm}(\omega) \end{bmatrix}.$$

By substituting this into equation (17), solutions are obtained (see reference (20) for a similar derivation) as

$$H_{kk}(\omega) = \left[\frac{D_k(\omega)}{D_{k-1}(\omega)}\right]^{\frac{1}{2}}, \qquad k = 1, 2, \ldots m, \tag{19}$$

where $D_k(\omega)$ is the kth principal minor of $S^0(\omega)$ with D_0 being defined as unity, and

$$H_{jk}(\omega) = H_{kk}(\omega)\,\frac{S^0\begin{pmatrix}1,2,\ldots,k-1,j\\1,2,\ldots,k-1,k\end{pmatrix}}{D_k(\omega)}, \quad k = 1, 2, \ldots m, \quad j = k+1, \ldots m, \tag{20}$$

where

$$S^0\begin{pmatrix}1,2,\ldots k-1,j\\1,2,\ldots k-1,k\end{pmatrix} = \begin{bmatrix} S^0_{11} & S^0_{12} & \ldots & S^0_{1,k-1} & S^0_{1k} \\ S^0_{21} & S^0_{22} & \ldots & S^0_{2,k-1} & S^0_{2k} \\ \ldots & \ldots & \ldots & \ldots & \ldots \\ S^0_{k-1,1} & S^0_{k-1,2} & \ldots & S^0_{k-1,k-1} & S^0_{k-1,k} \\ S^0_{j1} & S^0_{j2} & \ldots & S^0_{j,k-1} & S^0_{jk} \end{bmatrix}$$

is the determinant of a submatrix obtained by deleting all elements except the $(1, 2, \ldots k-1, j)$th row and $(1, 2, \ldots k-1, k)$th column of $S^0(\omega)$.

It is noted that the above solutions are valid only when the matrix $S^0(\omega)$ is Hermitian and positive definite, as can be seen from equation (19).

Because the cross-spectral density matrix $S^0(\omega)$ is known to be only non-negative definite, special consideration is needed in those cases where $S^0(\omega)$ has a zero principal

minor. This is discussed in Appendix II.

Since the real and the imaginary parts of cross-spectral density functions are respectively even and odd in ω, it can be shown from successive substitutions, with equations (19) and (20), that

$$\begin{aligned} \operatorname{Re} H_{jk}(\omega) &= \operatorname{Re} H_{jk}(-\omega), \\ \operatorname{Im} H_{jk}(\omega) &= -\operatorname{Im} H_{jk}(-\omega) \end{aligned} \tag{21}$$

for $j > k$, and

$$H_{jj}(\omega) = H_{jj}(-\omega) \geqslant 0,$$

from which it follows that $h_{jk}(\mathbf{x})$ is real.

If $H_{jk}(\omega)$ is written in polar form,

$$H_{jk}(\omega) = |H_{jk}(\omega)|\, e^{i\theta_{jk}(\omega)}, \tag{22}$$

then, due to equation (21), the argument $\theta_{jk}(\omega)$ is antisymmetric in ω; that is,

$$\theta_{jk}(\omega) = -\theta_{jk}(-\omega), \tag{23}$$

with $\theta_{jj}(\omega) = 0$.

Once $H(\omega)$ is computed by using equations (19) and (20), then, instead of passing a white noise vector through filters, the process $f_j(\mathbf{x})$ can be simulated in a more efficient way by the following series:

$$f_j(\mathbf{x}) = \sum_{m=1}^{j} \sum_{l=1}^{N} |H_{jm}(\omega_l)| \sqrt{2\Delta\omega}\, \cos\left[\omega_l' \cdot \mathbf{x} + \theta_{jm}(\omega_l) + \phi_{ml}\right], \tag{24}$$

where ω_l, ω_l', $\Delta\omega$ and N are as defined previously in equation (5) for n dimensional processes and

$$\theta_{jm}(\omega_l) = \tan^{-1}\left(\frac{\operatorname{Im} H_{jm}(\omega_l)}{\operatorname{Re} H_{jm}(\omega_l)}\right).$$

It then follows that the ensemble average $E[f_j(\mathbf{x})]$ is zero and the cross correlation $R_{jk}(\xi)$ with $j \geqslant k$ is

$$\begin{aligned} R_{jk}(\xi) &= E[f_j(\mathbf{x}) f_k(\mathbf{x} + \xi)] \\ &= \sum_{m=1}^{k} \sum_{l=1}^{N} \Delta\omega\, |H_{jm}(\omega_l)\, H_{km}(\omega_l)| \frac{1}{\Delta\omega'} \int_{-\frac{1}{2}\Delta\omega'}^{\frac{1}{2}\Delta\omega'} \cos\left[\omega' \cdot \xi + \theta_{jm}(\omega_l) - \theta_{km}(\omega_l)\right] \mathrm{d}(\delta\omega). \end{aligned} \tag{25}$$

In the same way as for equation (7), one can show that

$$\begin{aligned} &\frac{1}{\Delta\omega'} \int_{-\frac{1}{2}\Delta\omega'}^{\frac{1}{2}\Delta\omega'} \cos\left[\omega_l' \cdot \xi + \theta_{jm}(\omega_l) - \theta_{km}(\omega_l)\right] \mathrm{d}(\delta\omega) \\ &\qquad = \cos\left[\omega_l \cdot \xi + \theta_{jm}(\omega_l) - \theta_{km}(\omega_l)\right]. \end{aligned}$$

In addition, equation (25) is reduced to

$$R_{jk}(\xi) = \sum_{m=1}^{k} \sum_{l=1}^{N} |H_{jm}(\omega_l)\, H_{km}(\omega_l)|\, \Delta\omega \exp\left\{i\left[\omega_l \cdot \xi + \theta_{jm}(\omega_l) - \theta_{km}(\omega_l)\right]\right\} \tag{26}$$

with the aid of the following equation:

$$\sum_{l=1}^{N} |H_{jm}(\omega_l) H_{km}(\omega_l)| \, \Delta\omega \sin [\omega_l \cdot \xi + \theta_{jm}(\omega_l) - {}_{km}(\omega_l)]$$

$$= \int_{-\infty}^{\infty} |H_{jm}(\omega) H_{km}(\omega)| \sin [\omega \cdot \xi + \theta_{jm}(\omega) - \theta_{km}(\omega)] \, d\omega = 0. \tag{27}$$

In obtaining equation (27) use is made of the fact that the amplitude and the argument of the sine function of the integrand are respectively even and odd in ω because of equation (23).

Finally, letting $N \to \infty$, one obtains, in terms of equations (22) and (17),

$$R_{jk}(\xi) = \lim_{N \to \infty} \sum_{m=1}^{k} \sum_{l=1}^{N} H_{jm}(\omega_l) \bar{H}_{km}(\omega_l) \, \Delta\omega \exp (i\omega_l \cdot \xi)$$

$$= \int_{-\infty}^{\infty} \sum_{m=1}^{k} H_{jm}(\omega) \bar{H}_{km}(\omega) \exp (i\omega \cdot \xi) \, d\omega$$

$$= \int_{-\infty}^{\infty} S_{jk}^{0}(\omega) \exp (i\omega \cdot \xi) \, d\omega = R_{kj}^{0}(\xi). \tag{28}$$

Thus equation (28) shows that the processes $f_j(\mathbf{x})$ ($j = 1, \ldots m$), as simulated by equation (24), possess the target cross-correlation functions and hence the target cross-spectral density, with respect to an ensemble average.

4. SIMULATION OF MULTIDIMENSIONAL NON-HOMOGENEOUS PROCESSES

Simulations of non-stationary processes have been studied, mostly in connection with earthquake ground motion. The common feature of these studies is that a non-stationary process can be simulated by multiplying by an envelope function the stationary process generated either by filtering a white noise [3, 4, 5] or by a series of oscillations with random frequency and random phase [6, 7].

The efficient method of simulation that has been proposed here for multidimensional homogeneous processes can be directly generalized to a non-homogeneous process characterized by an evolutionary power spectrum as introduced by Priestley [21, 22].

As a background study, consider a general one-dimensional homogeneous process $f_0(x)$, which can always be expressed in the form of the spectral representation

$$f_0(x) = \int_{-\infty}^{\infty} e^{i\omega x} \, dz(\omega), \tag{29}$$

where $z(\omega)$, called the spectral process, is orthogonal in the sense that the increments $dz(\omega_1)$ and $dz(\omega_2)$ are uncorrelated when $\omega_1 \neq \omega_2$.

By employing the orthogonal condition of $z(\omega)$, the autocorrelation function of $f(x)$ is found to be

$$R_0(\xi) = \int_{-\infty}^{\infty} e^{i\omega\xi} E|dz(\omega)|^2. \tag{30}$$

Assume that the spectral density function $s_0(\omega)$ exists. Then $E|dz(\omega)|^2 = s_0(\omega)d\omega$, and equation (30) is reduced to the well-known Wiener–Khintchine relationship. For the case

when $f_0(x)$ is real, equation (29) becomes [19]

$$f_0(x) = \int_0^\infty [\cos \omega x \, dU(\omega) + \sin \omega x \, dV(\omega)], \tag{31}$$

where $U(\omega)$ and $V(\omega)$ for any $\omega \geqslant 0$ are two mutually orthogonal processes, both real and with orthogonal increments, such that

$$E[dU(\omega)]^2 = E[dV(\omega)]^2 = S_1{}^0(\omega)\, d\omega,$$

where $S_1{}^0(\omega)\,(= 2S_0(\omega))$ is the one-sided spectral density function.

It is pointed out that if one defines

$$dU(\omega_k) = [2S_1{}^0(\omega_k)\, \Delta\omega]^{\frac{1}{2}} \cos \phi_k,$$

$$dV(\omega_k) = [2S_1{}^0(\omega_k)\, \Delta\omega]^{\frac{1}{2}} \sin \phi_k, \tag{32}$$

where ω_k, $\Delta\omega$ and ϕ_k are as defined in equation (5), and recalls the fact that $\omega_k' \doteq \omega_k$, then all the conditions imposed on $U(\omega)$ and $V(\omega)$ are satisfied, and equation (5) is basically consistent with the spectral representation.

It is seen from equation (31) that a homogeneous process is additively built up by orthogonal oscillations with random amplitudes. This concept of orthogonal components can be extended to that of the oscillatory process $f_e{}^0(x)$, expressed as

$$f_e{}^0(x) = \int_0^\infty B(x, \omega)[\cos \omega x \, dU(\omega) + \sin \omega x \, dV(\omega)], \tag{33}$$

where $B(x, \omega)$ is a deterministic modulating function characterizing the "non-homogeneity" of the process, and $U(\omega)$ and $V(\omega)$ are the same as defined in equation (31).

By using the orthogonal conditions of $U(\omega)$ and $V(\omega)$, the mean square of $f_e{}^0(x)$ is found to be

$$E[f_e{}^0(x)]^2 = \int_0^\infty B^2(x, \omega)\, s_1{}^0(\omega)\, d\omega = \int_0^\infty S_e{}^0(x, \omega)\, d\omega, \tag{34}$$

where $S_e{}^0(x, \omega) = B^2(x, \omega)\, S_1{}^0(\omega)$ is defined as the evolutionary power spectral density function.

For the detailed discussion and the estimation of the evolutionary power spectrum, readers are referred to references [11] and [12].

The direct generalization of the above discussion to n-dimensional processes is obvious. Thus, if a real non-homogeneous process has an evolutionary power spectral density function, the process $f_e{}^0(\mathbf{x})$ can be simulated by

$$f_e{}^0(\mathbf{x}) = \sqrt{2} \sum_{k=1}^{N} [B^2(\mathbf{x}, \boldsymbol{\omega}_k)\, S_0(\boldsymbol{\omega}_k)\, \Delta\boldsymbol{\omega}]^{\frac{1}{2}} \cos (\boldsymbol{\omega}_k' \cdot \mathbf{x} + \phi_k), \tag{35}$$

where $B(\mathbf{x}, \boldsymbol{\omega})$ is the n-dimensional modulating function and the remaining notations are the same as in the case of a homogeneous process given by equation (5). It can be shown that the simulated $f_e(\mathbf{x})$ possesses the target evoluationary power spectrum as $N \to \infty$.

Note that in a particular case when $B(\mathbf{x}, \omega) = B(\mathbf{x})$, then $f_e{}^0(\mathbf{x})$ can be obtained by multiplying a homogeneous process simulated from $S_0(\boldsymbol{\omega})$ by the spatial envelope function $B(\mathbf{x})$.

5. SIMULATION OF GENERALIZED FORCES

In performing either the normal mode analysis of linear structures or the modal analysis of non-linear structures in a Galerkin sense, one always deals with generalized forces. When the excitation is of a random nature, then the simulation of a generalized force plays an important role in the numerical solution, especially to the non-linear problems.

Consider a random excitation field $f(t, \mathbf{x})$ in which t is the time variable and $\mathbf{x} = (x_1, x_2, x_3)$ are the spatial coordinates. The generalized force corresponding to the nth mode $\mu_n(\mathbf{x})$ is written as

$$F_n(t) = \int_D f(t, \mathbf{x})\, \mu_n(\mathbf{x})\, d\mathbf{x}, \tag{36}$$

where D is the domain of integration.

Assume that $f(t, \mathbf{x})$ is a stationary homogeneous process. Then it can be simulated by equation (5) with dimension = 4:

$$f(t, \mathbf{x}) = \sqrt{2} \sum_{i=1}^{N_1} \sum_{j=1}^{N_2} \sum_{k=1}^{N_3} \sum_{l=1}^{N_4} A_{ijkl} \cos(\omega_i' t + \lambda_j' x_1 + h_k' x_2 + k_l' x_3 + \phi_{ijkl}), \tag{37}$$

where the notations are corresponding to the ones specified in equation (5).

Substituting equation (37) into equation (36), one obtains

$$F_n(t) = \sqrt{2} \sum_{i=1}^{N_1} (G_{ni} \cos \omega_i' t - H_{ni} \sin \omega_i' t), \tag{38}$$

where

$$G_{ni} = \sum_{j=1}^{N_2} \sum_{k=1}^{N_3} \sum_{l=1}^{N_4} A_{ijkl}(B_{njkl} \cos \phi_{ijkl} - D_{njkl} \sin \phi_{ijkl}),$$

$$H_{ni} = \sum_{j=1}^{N_2} \sum_{k=1}^{N_3} \sum_{l=1}^{N_4} A_{ijkl}(B_{njkl} \sin \phi_{ijkl} + D_{njkl} \cos \phi_{ijkl}), \tag{39}$$

with

$$B_{njkl} = \int_D \cos(\lambda_j' x_1 + h_k' x_2 + k_l' x_3) \mu_n(\mathbf{x})\, d\mathbf{x},$$

$$D_{njkl} = \int_D \sin(\lambda_j' x_1 + h_k' x_3 + k_l' x_3)\, \mu_n(\mathbf{x})\, d\mathbf{x}. \tag{40}$$

It is pointed out that in many cases the integrations in equation (40) can be carried out in closed form. Furthermore, G_{ni} and H_{ni} as given in equation (39) are independent of time and need to be computed only once. Thus, the number of terms in the series is reduced from $N = N_1 N_2 N_3 N_4$ to N_1 in the subsequent numerical calculations in the time domain. No such advantage exists if equation (1) is used, because in that case the same number of terms that appeared in the simulation of the process will appear in the simulation of the generalized force.

However, the generalized force simulated by equation (38) is ergodic only at $N \to \infty$.

To see this, construct a random variable $\widetilde{F_n^2(t)}$ such that

$$\widetilde{F_n^2(t)} = \lim_{T\to\infty} \frac{1}{T}\int_0^T F_n^2(t)\,\mathrm{d}t$$

$$= \lim_{T\to\infty} \frac{2}{T}\sum_{i=1}^{N_1}\int_0^T [G_{ni}^2\cos^2\omega_i' t - 2G_{ni}H_{ni}\cos(\omega_i' t)\sin\omega_i' t$$

$$+ H_{ni}^2\sin^2\omega_i' t]\,\mathrm{d}t + 2\sum_{i=2}^{N_1}\sum_{j=1}^{i-1}\int_0^T [G_{ni}G_{nj}\cos(\omega_i' t)\cos\omega_j' t$$

$$- 2G_{nk}H_{nj}\cos(\omega_i' t)\sin\omega_j' t + H_{ni}H_{nj}\sin(\omega_i' t)\sin\omega_j' t]\,\mathrm{d}t.$$

Performing the integration and taking the limit, one can show that

$$\widetilde{F_n^2(t)} = \sum_{i=1}^{N_1}(G_{ni}^2 + H_{ni}^2).$$

Since G_{ni} and H_{ni} are functions of random phases ϕ_{ijkl}, $\widetilde{F_n^2(t)}$ is a random variable which can be shown to converge in mean square to $E[\widetilde{F_n^2(t)}]$ as $N_1 \to \infty$ with

$$E[\widetilde{F_n^2(t)}] = \sum_{i=1}^{N_1}[EG_{ni} + EH_{ni}]$$

$$= \sum_{i=1}^{N_1}\sum_{j=1}^{N_2}\sum_{k=1}^{N_3}\sum_{l=1}^{N_4} A_{ijkl}^2[B_{njkl}^2 + D_{njkl}^2]. \tag{41}$$

The ergodicity is important in the time domain analysis. Therefore the above approach is improved in what follows so that the simulated generalized force is ergodic for any finite number of N_1.

Consider M generalized forces corresponding to M modes, with each of them expressed as in equation (38); then the cross correlation among them can be shown (Appendix III) to be

$$R_{mn}(\tau) = \sum_{i=1}^{N_1}[C_{mni}\cos\omega_i\tau + Q_{mni}\sin\omega_i\tau], \tag{42}$$

where

$$C_{mni} = \sum_{j=1}^{N_2}\sum_{k=1}^{N_3}\sum_{l=1}^{N_4} A_{ijkl}^2(B_{mjkl}B_{njkl} + D_{mjkl}D_{njkl}),$$

$$Q_{mni} = \sum_{j=1}^{N_2}\sum_{k=1}^{N_3}\sum_{l=1}^{N_4} A_{ijkl}^2(B_{mjkl}D_{njkl} - B_{njkl}D_{mkjl}). \tag{43}$$

If the cross spectral density function $S_{mn}(\omega)$ between $F_m(t)$ and $F_n(t)$ is written as

$$S_{mn}(\omega) = C_{mn}(\omega) - iQ_{mn}(\omega),$$

it follows that

$$R_{mn}(\tau) = \int_{-\infty}^{\infty}[C_{mn}(\omega)\cos\omega\tau + Q_{mn}(\omega)\sin\omega\tau]\,\mathrm{d}\omega. \tag{44}$$

Comparison of equations (42) and (44) indicates the following relation:

$$S_{mn}(\omega_l) = \frac{1}{\Delta\omega}(C_{mnl} - iQ_{mnl}). \tag{45}$$

Note that, from equation (43),

$$Q_{mnl} = -Q_{nml},$$

$$Q_{nnl} = 0.$$

Thus the cross spectral density matrix of the generalized forces is Hermitian as it should be.

From equation (42) one obtains

$$R_{nn}(0) = \sum_{i=1}^{N_1}\sum_{j=1}^{N_2}\sum_{k=1}^{N_3}\sum_{l=1}^{N_4} A_{ijkl}(B_{njkl}^2 + D_{njkl}^2) = E[\widetilde{F_n^2(t)}].$$

This is consistent with equation (41) as expected.

With the cross spectral density matrix thus obtained, $F_n(t)$ $(n = 1, 2, \ldots, M)$ can be easily simulated as an M-component multivariate process as described in section 3.

6. CONCLUSION

Efficient methods are presented for digital simulation of a general homogeneous process (multidimensional or multivariate or multivariate-multidimensional) as a series of cosine functions with weighted amplitudes, almost evenly spaced frequencies, and random phase angles. The approach is also extended to the simulation of a general non-homogeneous oscillatory process characterized by an evolutionary power spectrum. Generalized forces involved in the modal analysis of linear or non-linear structures can be efficiently simulated as a multivariate process by using the cross-spectral density matrix computed from the spectral density function of the multidimensional excitation process.

Possible applications include simulation of (i) wind-induced ocean wave elevation, (ii) spatial random variation of material properties, (iii) the fluctuating part of atmospheric wind velocities and, (iv) random surface roughness of highways and airport runways.

ACKNOWLEDGMENTS

This work was supported by the National Science Foundation under NSF–GK 3858 and GK 24925.

REFERENCES

1. M. SHINOZUKA 1971 *Journal of the Acoustical Society of America* **49,** 357–367. Simulation of multivariate and multi-dimensional random processes.
2. L. E. BORGMAN 1969 *Journal of Waterways and Harbors Division, Proceedings of the American Society of Civil Engineers* **WW4,** 556–583. Ocean wave simulation for engineering design.
3. M. SHINOZUKA and Y. SATO 1967 *Proceedings of the American Society of Civil Engineers* **93,** 11–40. Simulation of nonstationary random processes.
4. M. AMIN and A. H.-S. ANG 1968 *EMD Journal, American Society of Civil Engineers* **94,** 559–583. Nonstationary stochastic models of earthquake motions.
5. G. W. HOUSNER and P. C. JENNINGS 1964 *EMD Journal, Amrrican Society of Civil Engineers* **90,** 113–150. Generation of artificial earthquakes.
6. J. E. GOLDBERG, J. L. BOGDANOFF and D. R. SHARPE 1964 *Bulletin of the Seismological Society of America* **54,** 263–276. The response of simple non-linear structure to a random disturbance of earthquake type.

7. M. SHINOZUKA and P. W. BRANT 1969 *Proceedings of the American Society of Civil Engineers—EMD Speciality Conference on Probabilistic Concepts and Methods in Engineering at Purdue University,* 12–14 *November* 1969 pp. 42–46. Applications of evolutionary power spectrum in structural dynamics.
8. M. SHINOZUKA and C. J. ASTILL 1972 *American Institute of Aeronatuics and Astronautics Journal* **10,** 456–462. Random eigenvalue problems in structural mechanics.
9. M. SHINOZUKA and Y.-K. WEN 1972 *American Institute of Aeronautics and Astronautics Journal* **10,** 37–40. Monte Carlo solution of nonlinear vibrations.
10. M. SHINOZUKA and Y.-K. WEN 1971 *Proceedings of the International Symposium of Stochastic Hydraulics, Pittsburgh, 31 May–2 June 1971* pp. 507–521. Nonlinear dynamic analysis of offshore structures; a Monte Carlo approach.
11. C. J. ASTILL, S. B. NOSSEIR and M. SHINOZUKA 1972 *Journal of Structural Mechanics* **1,** No. 1 (in press). Impact loading on structures with random properties.
12. R. VAICAITIS and C.-M. JAN 1972 *American Institute of Aeronautics and Astronautics Journal* **10,** 895–899. Nonlinear panel response and noise transmission from a turbulent boundary layer by a Monte Carlo approach.
13. Y. K. WEN and M. SHINOZUKA 1972 *Journal of Waterways, Harbors and Coastal Engineering Division, Proceedings of the American Society of Civil Engineers* **98,** 177–190. Analysis of floating plate under ocean waves.
14. Y. -K. WEN and M. SHINOZUKA 1971 *Proceedings of the Third International Conference on Wind Effects in Buildings and Structures, Tokyo, Japan, 6–11 September 1971* pp. 421–428. Monte Carlo solution of structural response to wind load.
15. H. ITAGAKI and M. SHINOZUKA 1971 *NSF GK 3858/24925 Technical Report No. 16, Columbia University, June 1971.* Application of Monte Carlo technique to fatigue failure analysis under random loading. (To be published in an ASTM Special Technical Publication No. 411).
16. R. N. IYENGAR and M. SHINOZUKA 1972 *International Journal of Earthquake Engineering and Structural Dynamics* **1,** 69–78. Effects of self-weight and vertical acceleration on the behaviour of tall structures during earthquake.
17. S. BOCHNER 1959 *Lectures on Fourier Integrals.* Princeton University Press. See pp. 325–328. (English translation by M. Tenebaum and H. Pollard.)
18. S. O. RICE 1954 In *Selected Papers on Noise and Stochastic Processes* (Editor: N. Wax). Mathematical analysis of random noise. New York: Dover Publications Inc. See pp. 180–181.
19. H. CRAMER and M. R. LEADBETTER 1967 *Stationary and Related Stochastic Processes.* New York: Wiley. See p. 161 and p. 135.
20. F. R. GANTMACHER 1960 *The Theory of Matrices, Volume* 1. New York: Chelsea. See p. 37.
21. M. B. PRIESTLEY 1965 *Journal of the Royal Statistical Society B.*27, 204–236. Evolutionary spectra and nonstationary processes.
22. M. B. PRIESTLEY 1967 *Journal of Sound and Vibration* **6,** 86–97. Power spectral analysis of non-stationary random processes.

APPENDIX I

To investigate the rate of convergence of $R(\xi)$ to $R_0(\xi)$, consider a one-dimensional process with the one-sided spectral density $S_0(\omega)$ specified in the region $0 \leqslant \omega \leqslant \omega_u$; otherwise $S_0(\omega) = 0$.

For this case, equations (8) and (9) are written, respectively, as

$$R(\xi) = \sum_{k=1}^{N} S_0(\omega_k)\,\Delta\omega \cos \omega_k \xi, \tag{A1}$$

with $N = \omega_u/\Delta\omega$, and

$$R_0(\xi) = \int_0^{\omega_u} S_0(\omega) \cos \omega\xi \, d\omega. \tag{A2}$$

By using a Taylor series expansion, and neglecting the higher order terms of $(\Delta\omega)$, equation (A2) can be expressed as

$$R_0(\xi) = \sum_{k=1}^{N} S_0(\omega_k)\,\Delta\omega \cos \omega_k \xi + \frac{(\Delta\omega)^3}{24} \sum_{k=1}^{N} [S_0(\omega_k) \cos \omega_k \xi]''$$

where

$$[\ ]'' \equiv \frac{d^2}{d\omega^2}[\ ].$$

If the last term of the above expression is approximated by $\{(\Delta\omega)^2/24\}[S_0(\omega_u)\cos\omega_u\xi]'$, then equation (A2) together with equation (A1) produces

$$R_0(\xi) - R(\xi) = \frac{\omega_u^2}{24N^2}[S_0'(\omega_u)\cos\omega_u\xi - \xi S_0(\omega_u)\sin\omega_u\xi].$$

This shows that the autocorrelation function $R(\xi)$ of the simulated process converges as $1/N^2$ to the target function $R_0(\xi)$.

To examine the convergence in the frequency domain, apply the Wiener–Khintchine relationship to equation (A1):

$$S(\omega) = \frac{1}{\pi}\sum_{k=1}^{N} S_0(\omega_k)\,\Delta\omega\int_0^\infty \cos\omega_k\xi\cos\omega\xi\,d\xi = \sum_{k=1}^{N} S_0(\omega)\,\Delta\omega\delta(\omega-\omega_k).$$

The spectral distribution $\Gamma(\omega)$ of $f(x)$ in this case is

$$\Gamma(\omega) = \int_0^\omega S_0(\omega)\,d\omega \doteq \sum_{k=1}^{N(\omega)} S_0(\omega_k)\,\Delta\omega,$$

where $N(\omega)$ is the number of ω_k such that $\omega_k \leqslant \omega$.

With $\Gamma(\omega)$ thus defined, one can write

$$\Gamma(\omega+\Delta\omega) - \Gamma(\omega) = S_0(\omega_{N(\omega)+1})\,\Delta\omega. \tag{A3}$$

By writing $\omega_{N(\omega)+1} = \omega + \alpha\Delta\omega$ with α ranging from 0 to 1 depending on the value of ω, equation (A3) can be expanded as

$$\Gamma(\omega+\Delta\omega) - \Gamma(\omega) = S_0(\omega)\,\Delta\omega + S_0'(\omega)\,\alpha(\Delta\omega)^2 + S_0''(\omega)\frac{\alpha^2(\Delta\omega)^3}{2} + \ldots.$$

For the target spectral distribution $\Gamma_0(\omega)$,

$$\Gamma_0(\omega+\Delta\omega) - \Gamma_0(\omega) = S_0(\omega)\,\Delta\omega + S_0'(\omega)\frac{(\Delta\omega)^2}{2} + S_0''(\omega)\frac{(\Delta\omega)^3}{6} + \ldots.$$

Therefore

$$[\Gamma_0(\omega+\Delta\omega) - \Gamma_0(\omega)] - [\Gamma(\omega+\Delta\omega) - \Gamma(\omega)]$$
$$= S_0'(\omega)(\Delta\omega)^2\left(\frac{1}{2}-\alpha\right) + S_0''(\omega)(\Delta\omega)^3\left(\frac{1}{6}-\frac{\alpha^2}{2}\right) + \ldots. \tag{A4}$$

For the purpose of normalization, one can let $\Gamma_0(\omega+\Delta\omega) - \Gamma_0(\omega) = S_0(\omega)\,\Delta\omega$. Then it follows from equation (A4) that

$$\frac{[\Gamma_0(\omega+\Delta\omega) - \Gamma_0(\omega)] - [\Gamma(\omega+\Delta\omega) - \Gamma(\omega)]}{\Gamma_0(\omega+\Delta\omega) - \Gamma_0(\omega)}$$
$$= \frac{1}{S_0(\omega)}\left[\frac{S_0'(\omega)\,\omega_u}{N}\left(\frac{1}{2}-\alpha\right) + \frac{S_0''(\omega)}{N^2}\omega_u^2\left(\frac{1}{6}-\frac{\alpha^2}{2}\right)\right]. \tag{A5}$$

Equation (A5) indicates that, in the interval $\Delta\omega$, the spectral density $S(\omega)$ converges on the average as $1/N^2$, to the target spectral density, since α has a mean value of 1/2.

APPENDIX II

Expanding equation (17), with $H(\omega)$ being a lower triangular matrix, one obtains

$$S^0_{jk} = H_{j1}\bar{H}_{k1} + H_{j2}\bar{H}_{k2} + \ldots H_{jk}\bar{H}_{kk}, \quad \text{for} \quad k < j,$$

$$S^0_{jj} = |H_{j1}|^2 + |H_{j2}|^2 + \ldots |H_{jj}|^2. \tag{B1}$$

From equations (24) and (B1) one can see that the jth component process is simulated from $H_{jk}(\omega)$ $(k = 1, 2, \ldots j)$ and that the coherence between the jth component and the kth component with $k < j$ is generated by $H_{jl}(\omega)$ and $H_{kl}(\omega)$ $(l = 1, 2, \ldots k)$. When a vanishing principal minor is due to a zero mean square density of, say, the jth component process at a wave number ω, then the elements of the cross-spectral density associated with this component are also zero at this particular wave number. It is easy to show that a sufficient condition for this case is

$$H_{jk}(\omega) = 0, \quad \text{for} \quad k = 1, 2, \ldots j,$$

$$H_{kj}(\omega) = 0, \quad \text{for} \quad k = j + 1, \ldots m.$$

The remaining elements of $H_{jk}(\omega)$ are then determined from the submatrix obtained by deleting the jth row and the jth column from $S^0(\omega)$.

A coherence of unity between two component processes (the jth and the $(j + 1)$th) at a wave number ω will also give rise to vanishing principal minors. This implies the complete linear dependence at this wave number between the two processes and hence the existence of the transfer function $\alpha(\omega)$ such that

$$S^0_{j+1,j+1}(\omega) = |\alpha(\omega)|^2 S^0_{jj}(\omega),$$

$$S^0_{j,j+1}(\omega) = \alpha(\omega) S^0_{jj}(\omega).$$

Therefore, at this ω, it can be shown that $S^0(\omega)$ will take the following form:

$$\begin{bmatrix} S^0_{11} \ldots S^0_{1j} & S^0_{1,j+1} \ldots S^0_{1m} \\ \ldots\ldots\ldots\ldots\ldots & \ldots\ldots\ldots\ldots\ldots \\ S^0_{j1} \ldots S^0_{jj} & S^0_{j,j+1} \ldots S^0_{jm} \\ S^0_{j+1,1} \ldots S^0_{j+1,j} & S^0_{j+1,j+1} \ldots S^0_{j+1,m} \\ \ldots\ldots\ldots\ldots\ldots & \ldots\ldots\ldots\ldots\ldots \\ S^0_{m1} \ldots S^0_{mj} & S^0_{mj+1} \ldots S^0_{mm} \end{bmatrix} = \begin{bmatrix} S^0_{11} \ldots S^0_{1j} & \alpha S^0_{1j} \ldots S^0_{1m} \\ \ldots\ldots\ldots\ldots\ldots & \ldots\ldots\ldots\ldots\ldots \\ S^0_{j1} \ldots S^0_{jj} & \alpha S^0_{jj} \ldots S^0_{jm} \\ \bar{\alpha} S^0_{j1} \ldots \bar{\alpha} S^0_{jj} & |\alpha|^2 S^0_{jj} \ldots \bar{\alpha} S^0_{jm} \\ \ldots\ldots\ldots\ldots\ldots & \ldots\ldots\ldots\ldots\ldots \\ S^0_{m1} \ldots S^0_{mj} & \alpha S^0_{mj} \ldots S^0_{mm} \end{bmatrix}.$$

In this case, $H(\omega)$ can be solved for this particular wave number ω in the following fashion.

First, reduce the size of both matrices $S^0(\omega)$ and $H(\omega)$ by deleting their $(j + 1)$th row and $(j + 1)$th column, then solve for the reduced $H(\omega)$ from the reduced $S^0(\omega)$, by way of equations (19) and (20). Finally, the deleted elements of $H(\omega)$, as can be seen by direct substitution in equation (B1), are given by

$$H_{j+1,k} = \bar{\alpha} H_{jk}, \quad \text{for} \quad k = 1, 2, \ldots, j,$$

$$H_{j+1,j+1} = 0,$$

$$H_{k,j+1} = 0, \qquad \text{for} \quad k = j + 2, \ldots, m.$$

If two component processes, again, say, the jth and the $(j+1)$th, are completely correlated, then $\alpha(\omega)$ as defined for the previous case will reduce to a real constant α_0 independent of wave numbers. This will lead to $D_k(\omega) = 0$, $k = j+1, j+2, \ldots, m$, for all wave numbers. For this case, it is necessary to simulate only $m-1$ component processes with the $(j+1)$th removed from the system, since it can be obtained by

$$f_{j+1}(\mathbf{x}) = \alpha_0 f_j(\mathbf{x}).$$

With the proper combination of the above procedures, it is possible to deal with the following situations: (i) more than one component of $S^0(\omega)$ vanishes; (ii) more than two components are completely coherent or completely correlated; (iii) the combination thereof.

APPENDIX III

The derivation of the form given in equation (42) for the cross correlation $R_{mn}(\tau)$ can be accomplished as follows.

$$\begin{aligned} R_{mn}(\tau) = E[F_m(t)\,F_n(t+\tau)] = 2\sum_{i=1}^{N_1}\sum_{j=1}^{N_1} \{&E[G_{mi}G_{nj}]\,E[\cos(\omega_i' t)\cos\omega_j'(t+\tau)] \\ &+ E[H_{mi}H_{nj}]\,E[\sin(\omega_i' t)\sin\omega_j'(t+\tau)] \\ &- E[G_{mi}H_{nj}]\,E[\cos(\omega_i' t)\sin\omega_j'(t+\tau)] \\ &- E[H_{mi}G_{nj}]\,E[\sin(\omega_i' t)\cos\omega_j'(t+\tau)]\}, \end{aligned} \tag{C1}$$

where

$$\begin{aligned} E[G_{mi}G_{nj}] = \sum_{p=1}^{N_2}\sum_{q=1}^{N_3}\sum_{r=1}^{N_4}\sum_{s=1}^{N_2}\sum_{t=1}^{N_3}\sum_{u=1}^{N_4} A_{ipqr}A_{jstu}\{&B_{mpqr}B_{nstu}\,E[\cos\phi_{ipqr}\cos\phi_{jstu}] \\ &+ D_{mpqr}D_{nstu}E[\sin\phi_{ipqr}\sin\phi_{jstu}] - B_{mpqr}D_{nstu}E[\cos\phi_{ipqr}\sin\phi_{jstu}] \\ &- B_{npqr}D_{mstu}E[\sin\phi_{ipqr}\cos\phi_{jstu}]\} \\ = \frac{1}{2}\delta_{ij}\sum_{p=1}^{N_2}\sum_{q=1}^{N_3}\sum_{r=1}^{N_4} A_{ipqr}^2(&B_{mpqr}B_{npqr} + D_{mpqr}D_{npqr}), \end{aligned}$$

and, similarly, one can show that

$$E[H_{mi}H_{nj}] = E[G_{mi}G_{nj}]$$

and

$$E[H_{mi}G_{nj}] = -E[G_{mi}H_{nj}].$$

Equation (C1) is then reduced to

$$\begin{aligned} R_{mn}(\tau) &= 2\sum_{i=1}^{N_1}\{E[G_{mi}G_{ni}]\,E[\cos(\omega_i' t)\cos\omega_j'(t+\tau) + \sin(\omega' t)\sin\omega_j'(t+\tau)] \\ &\quad - E[G_{mi}H_{ni}]\,E[\cos(\omega_i' t)\sin\omega_j'(t+\tau) - \sin(\omega_i' t)\cos\omega_j'(t+\tau)]\} \\ &= 2\sum_{i=1}^{N_1}\{E[G_{mi}G_{ni}]\,E[\cos\omega_i'\tau] - E[G_{mi}H_{ni}]\,E[\sin\omega_i'\tau]\}. \end{aligned}$$

As in equation (7), it can be shown that

$$E[\cos\omega_i'\tau] = \cos\omega_i\tau$$

and

$$E[\sin\omega_i'\tau] = \sin\omega_i\tau.$$

Finally, $R_{mn}(\tau)$ takes the form of equation (42).